Frequency domain LPV controller synthesis for a positioning system with uncertain scheduling parameters ⋆

Philippe Schuchert and Alireza Karimi ⋆⋆

Laboratoire d'Automatique
École Polytechinique Fédérale de Lausanne (EPFL), Switzerland

Abstract: Ever-increasing demands from the industry require better performance out of the same system to achieve a competitive advantage. In systems functioning at different operating points, a fundamental trade-off between robustness and performance can limit the achieved performance. Linear Parameter Varying (LPV) controller synthesis can overcome this issue by adapting the controller parameters with the operating points. This requires a parametric LPV model of the system, which in many cases is difficult or costly to obtain. Recently, LPV controller design methods based on the frequency-domain data in different operating points have shown to result in great performance without the need of a parametric LPV model. In these approaches, however, the scheduling parameters are assumed to be measured exactly. In this paper, a new approach is proposed to design LPV controllers with slowly varying uncertain scheduling parameters, using only the frequency response data of a SISO system around different operating points. The proposed approach is applied on a rotary table, a machine used in the manufacturing industry. The dynamics of the rotary table depend on the inertia of the object mounted on-top which cannot be directly measured. Since the scheduling parameter cannot be measured, it is estimated using a short sequence of data that leads to an inexact estimation with interval uncertainty. For the system considered, the LPV controller designed by the proposed approach shows clear improvement over the state-of-the-art robust controller synthesis approaches.

1. INTRODUCTION

Rotary tables are systems used in the manufacturing industry to inspect machined objects, to assess if they are up to the desired specifications. A single rotary table must be able to rotate objects with small and large weights, and thus such a system can encounter a relatively broad set of dynamics during routine operation. A state-of-the-art robust control law can account for these varying dynamics, but may fail to achieve the desired control performance.

To obtain improved performance over traditional control strategies, control design schemes incorporating parameter-dependent gains (Rugh and Shamma, 2000) have been used to design non-linear controllers using the formalism of linear controller synthesis, with many reported successful applications (Hoffmann and Werner, 2015). In *Divide-and-conquer* gain-scheduling, the non-linear control law is obtained by interpolating between local controllers, e.g., Symens et al. (2004); Paijmans et al. (2006); da Silva et al. (2009); Dong et al. (2015). This requires tuning a possibly large number of different controllers, and the interpolation step can lead to loss of performance between operating points. LPV controller synthesis offers a compelling alternative to gain-scheduling method, e.g. Steinbuch et al. (2003); Wassink et al. (2005), but requires an LPV model of the system. In many cases, the LPV model is obtained by interpolating local models (Tóth et al., 2011).

An accurate LPV model is paramount to a good control design, but obtaining a parametric model is often difficult and expensive. For mechanical systems such as a rotary table, frequency response function (FRF) has been a proven tool to model the dynamics (Oomen, 2018), and is relatively easy to obtain. For LPV systems, obtaining the FRF at different operating points can be used as an accurate representation of the system's local dynamics. Different FRF based controller synthesis approaches have been extended to parameter-dependent or LPV systems (Kunze et al., 2007; Karimi and Emedi, 2013; Bloemers et al., 2019a,b, 2021; Schuchert and Karimi, 2023), thus largely bypassing the costly modelling phase when using an LPV model. In these methods, it is assumed that the rate-of-change of the operating point is changing sufficiently slowly, as stability for fixed parameters implies stability for sufficient slowly varying parameters (Mohammadpour and Scherer, 2012). Moreover, it is assumed, often implicitly, that the operating points, and therefore scheduling parameters, are known to a sufficiently high accuracy.

For the rotary table, during a routine day, objects of different shape, size, and weight will be inspected, resulting in different rotational inertias, and ultimately leading to parameter dependent dynamics. For this system, once an object is installed, the parameters do not change until the next item is inspected (piece-wise constant parameter). After changing an object, a precise value of the rotational inertia could be obtained from measurements by conducting a specific experiment, but obtaining this value is a time-consuming task, and must be repeated

⋆ This work is supported by INNOSUISSE under grant 48289.1 IP-ENG
⋆⋆Corresponding author: alireza.karimi@epfl.ch

every time a different object is inspected. This represents added costs for the machine operator and therefore is not desired. On the other hand, it is often possible to derive an estimate of the rotational inertia from input/output data of the rotary table system. However, this estimate is often inexact, and the uncertainty must be considered during controller synthesis. In the parametric case, the absence of exact knowledge of the operating point has been studied (Kose and Jabbari, 1999; Sato et al., 2010; Agulhari et al., 2013), although this problem has not been studied in FRF-based LPV approaches.

We propose an extension to the method proposed in Schuchert and Karimi (2023), when the scheduling parameters are uncertain, but slowly varying. The resulting synthesis problem is convex in the controller-parameters, and is formulated as a semi-infinite program (SIP). This SIP is sampled, and solved with an off-the-shelf convex solver. An industrial rotary table system is considered to highlight the applicability of the proposed method and improvements over the state-of-the-art control design strategies.

This paper is organized as follows: in Section 2, a description of the system and problem to be solved is given. In Section 3, a solution by convex optimization using only the frequency response of the system is presented. In Section 4, implementation considerations are discussed. Experimental results using a real rotary table illustrate the effectiveness of the approach in Section 5. The paper ends with some concluding remarks.

Notation: The imaginary unit is denoted $j = \sqrt{-1}$. The conjugate transpose of a complex vector F is denoted by F^* and its Euclidean norm by $|F| = \sqrt{F^*F}$. The $\mathcal{H}_2$ and $\mathcal{H}_\infty$ norm of an LTI system are denoted $\|\cdot\|_2$ and $\|\cdot\|_\infty$, respectively.

2. PROBLEM STATEMENT

2.1 System Description

A rotary table consists of a DC motor connected to a rotating plate through a gear train. Two sensors are available: a tachometer to measure the angular speed of the motor, and an incremental encoder to precisely measure the plate's angular position. A picture of the set-up is shown in Fig. 1. The system has to accurately position objects with weights ranging from one to hundreds of kilograms. This large variation in the payload results in a significant change of the system dynamics. The dynamics depend on the inertia of the inspected object, which cannot be directly measured. Measurable quantities such as the object's mass or its position are not a complete description of the inertia, and using the aforementioned quantities in the scheduling parameters only increases the complexity of the overall problem. In this paper, we propose to use an estimate of the operating point based on a short sequence of data (around 2 sec) before starting the inspection in an initialization phase. Since the data is noisy and the data length is short, the estimate will not be exact. Therefore, it is assumed that only an estimate $\hat{\mathsf{p}}$ of the operating point p is available:

$$\hat{\mathsf{p}} := \mathsf{p} + \delta, \quad \delta \in \mathbb{D} \tag{1}$$

where $\mathbb{D}$ describes the uncertainty in the estimation. In case the operating point can be accurately measured, $\mathbb{D}$ is a single point, namely $\mathbb{D} := \{0\}$.

Fig. 1. Rotary table. A metallic frame is installed on-top of the rotary table, where various weights can be installed at different positions. During a routine day, objects of different shape, size, and weight will be inspected, resulting in parameter dependent dynamics.

In industry, a common control scheme for such systems is cascaded control loops: the inner-loop regulates the motor angular speed and the outer-loop the disk angular position. We will adopt the same control architecture, and assume that the inner-loop is already tuned. The inner-loop is relatively insensitive to the weights of the objects mounted on-top due to a large reduction-ratio in the gear-train. Therefore, a single robust control law achieves adequate performance. The model of the outer-loop, with the inner-loop closed, is denoted

$$G_{\mathsf{p}} = \frac{\mathcal{G}_{\mathsf{p}} K_m}{1 + \mathcal{G}_{\mathsf{p}} K_m},$$

where $\mathcal{G}_{\mathsf{p}}$ is a single-input two-output system representing the rotary table dynamics and K_{m} the inner-controller. For the outer-loop, to obtain improved performance over state-of-the-art synthesis, it is desired to design an LPV controller. The outer-loop controller to be designed is denoted $K_{\hat{\mathsf{p}}}$, and a block diagram representing this interconnection can be found in Fig. 2.

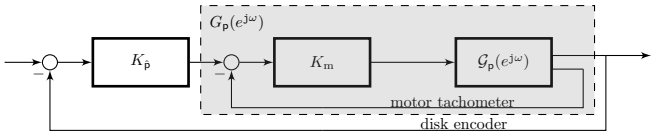

Fig. 2. Block diagram of the control loop architecture

The system of interest can be *locally*, i.e., around each operating point p, well approximated by an LTI system. It is usually assumed that the frozen dynamics representation at each operating point remains a valid description of the system. This assumption is clearly valid in this application, as once an object is mounted on-top of the rotating plate, the operating point does not change. At every operating point, a unique frequency response function $G_{\mathsf{p}}(e^{j\omega})$ exists, which can be used to model the (frozen) dynamics (Tóth, 2010). The frequency set is chosen as $\omega \in \Omega_{G_{\mathsf{p}}} := (-\pi/T_s,\, \pi/T_s] \setminus B_{G_{\mathsf{p}}}$, where $B_{G_{\mathsf{p}}}$ is the set of frequencies corresponding to the poles of G_{p} on

the unit circle. The FRF can be obtained directly from spectral identification methods (Pintelon and Schoukens, 2012), avoiding the costly parametric identification phases (structure identification, parameter estimation and model validation).

2.2 Frequency Response Data

Twenty-five local data sets are collected around different operating points, by varying weights and the positions of the object on the rotary table. Each data set consists of $T = 4000$ input and output measurements sampled at $T_s = 5 \cdot 10^{-3}$ s. The input r is a *sum-of-sines* signal with random phase given by:

$$r_t = \sum_{k=1}^{T/2} \left(\alpha + \frac{\beta}{k}\right) \sin(2\pi k(t - \tau_k)/T)$$

where τ_k is a random integer in $\{0, \dots, T-1\}$ and α, β constants to shape the reference signal spectrum. The constant $\alpha > 0$ is chosen sufficiently large to excite well all frequencies, but not too large to saturate the input of the DC motor. The constant $\beta > 0$ is chosen to add additional excitation in low frequencies. The frequency response function (FRF) computed at each of the 25 operating points at 500 logarithmically spaced frequency points in $\{1, \pi/T_s\}$, and is shown in Fig. 3. The color of the FRF is changing linearly with the frequency of the first resonance peak ω_{peak}. Due to a relatively sharp first resonance peak in the dynamics, if the operating point is not well measured or estimated, poor closed-loop performance may be achieved.

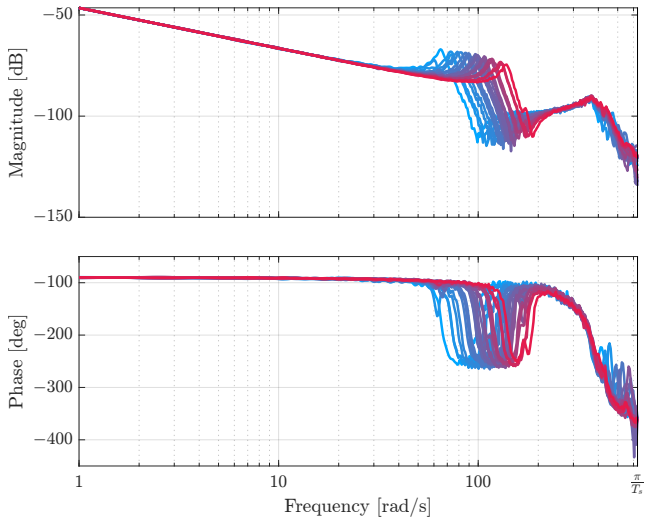

Fig. 3. Frequency response of the system around different operating points. The color of the FRF is chosen according to the frequency of the first resonance peak.

2.3 Operating point

Different combinations of weights and positions can result in very similar dynamics, e.g., large weights near the center or small weights far away from it may both have the same rotational inertia. Instead of using the rotational inertia as operating point, it is proposed to use the frequency corresponding to the first resonance peak in the open-loop FRF as a proxy, i.e. $\mathsf{p} := \omega_{\text{peak}}$. In first approximation, the transmission and rotating disk can be reasonably well modeled by a mass-spring-damper system:

$$(J_{\text{rotary}} + J_{\text{object}})\ddot{y}_{\text{disk}} = -b\dot{y}_{\text{disk}} - k y_{\text{disk}} + kR y_{\text{motor}} \quad (2)$$

where J_{rotary} is the no-load inertia and J_{object} the added inertia from the object inspected. b, k are friction and spring constants, and R is the transmission ratio. The angular position of the disk and motor are denoted y_{disk} and y_{motor}, respectively. The peak frequency of this system is given by

$$\omega_{\text{peak}} = \sqrt{\frac{k}{J_{\text{rotary}} + J_{\text{object}}}} \quad (3)$$

The constants in (3) can be computed once precisely in a controlled environment if needed. Notably, the operating point $\mathsf{p} = \omega_{\text{peak}}$ belongs to the following set:

$$\mathbb{P} = \{\omega_{\text{peak}} \in \mathbb{R} \mid 65 \le \omega_{\text{peak}} \le 137\}$$

The operating point can clearly be obtained at the same time as identification is done, by simply reading of the corresponding frequency. On the workshop floor, performing a lengthy identification is not an acceptable solution (time-wise), and only a short experiment can be done to obtain a reasonable estimate $\hat{\mathsf{p}} = \hat{\omega}_{\text{peak}}$.

2.4 Synthesis objective

The inexact estimation of the operating point could be framed as uncertainty in the model dynamics, where each controller K_{p} should stabilize all models $G_{\mathsf{p}+\delta}$. This is not done, as it requires identifying additional models at the operating point $\mathsf{p} - \delta$. Instead, the synthesis objective is to design a SISO LTI controller $K_{\hat{\mathsf{p}}}$ such that $K_{\hat{\mathsf{p}}}$ stabilizes G_{p}, $\forall \delta \in \mathbb{D}, \forall \mathsf{p} \in \mathbb{P}$, and optimal w.r.t. a mixed-norm mixed-sensitivity problem:

$$\begin{aligned} &\min_{K_{\hat{\mathsf{p}}}} \max_{\mathsf{p}\in\mathbb{P},\delta\in\mathbb{D}} \|R_{\text{soft}}(G_{\mathsf{p}}, K_{\hat{\mathsf{p}}})\|_2 \\ &\text{subject to} \\ &\|R_{\text{hard}}(G_{\mathsf{p}}, K_{\hat{\mathsf{p}}})\|_\infty < 1. \end{aligned} \quad (4)$$

R_{soft} corresponds to non-critical objective(s) to be minimized, and defined as

$$R_{\text{soft}} = \begin{bmatrix} W_1 \mathcal{S}_{\mathsf{p}\hat{\mathsf{p}}} \\ W_2 \mathcal{U}_{\mathsf{p}\hat{\mathsf{p}}} \\ W_3 \mathcal{T}_{\mathsf{p}\hat{\mathsf{p}}} \end{bmatrix} \quad (5)$$

where the closed-loop transfer functions are defined as:

$$\mathcal{S}_{\mathsf{p}\hat{\mathsf{p}}} = \frac{1}{1 + G_{\mathsf{p}} K_{\hat{\mathsf{p}}}}, \; \mathcal{U}_{\mathsf{p}\hat{\mathsf{p}}} = \frac{K_{\hat{\mathsf{p}}}}{1 + G_{\mathsf{p}} K_{\hat{\mathsf{p}}}}, \; \mathcal{T}_{\mathsf{p}\hat{\mathsf{p}}} = \frac{G_{\mathsf{p}} K_{\hat{\mathsf{p}}}}{1 + G_{\mathsf{p}} K_{\hat{\mathsf{p}}}}$$

Similar to the problem formulation in Schuchert and Karimi (2023), R_{hard} are formulated as $\mathcal{H}_\infty$ constraints to shape individually the closed-loop transfer functions:

$$\|\underline{W_1}\mathcal{S}_{\mathsf{p}\hat{\mathsf{p}}}\|_\infty < 1, \quad \|\underline{W_2}\mathcal{U}_{\mathsf{p}\hat{\mathsf{p}}}\|_\infty < 1, \quad \|\underline{W_3}\mathcal{T}_{\mathsf{p}\hat{\mathsf{p}}}\|_\infty < 1 \;\; \forall \delta \in \mathbb{D}, \forall \mathsf{p} \in \mathbb{P} \quad (6)$$

or equivalently $R_{\text{hard}} = \text{diag}\{\underline{W_1}\mathcal{S}_{\mathsf{p}\hat{\mathsf{p}}}, \underline{W_2}\mathcal{U}_{\mathsf{p}\hat{\mathsf{p}}}, \underline{W_3}\mathcal{T}_{\mathsf{p}\hat{\mathsf{p}}}\}$.

3. LPV CONTROLLER SYNTHESIS

The following rational controller parametrization is considered:

$$K_{\hat{\mathsf{p}}} = \frac{X_{\hat{\mathsf{p}}}}{Y_{\hat{\mathsf{p}}}} = \frac{X_{\text{var}}}{Y_{\text{var}}} \frac{F_X}{F_Y}, \quad (7)$$

where $X_{\hat{\mathsf{p}}}$ and $Y_{\hat{\mathsf{p}}}$ are polynomials in the z-transform variable and F_X and F_Y are eventual fixed parts in the controller. X_{var} and Y_{var} are the variable parts of the controller, which should be optimized. They are functions of the estimated operating point via a user defined scheduling vector:

$$\theta(\hat{\mathsf{p}}) = [\theta_1(\hat{\mathsf{p}}),\ \ldots,\ \theta_{n_\theta}(\hat{\mathsf{p}})] \tag{8}$$

The controller numerator and denominator can be rewritten as

$$\begin{aligned} X_{\hat{\mathsf{p}}}(z) &= X_n(\hat{\mathsf{p}})z^n + \ldots + X_1(\hat{\mathsf{p}})z + X_0(\hat{\mathsf{p}}), \\ Y_{\hat{\mathsf{p}}}(z) &= \quad\ z^n\ + \ldots + Y_1(\hat{\mathsf{p}})z + \ Y_0(\hat{\mathsf{p}}), \end{aligned} \tag{9}$$

where

$$X_i(\hat{\mathsf{p}}) = \sum_{j=1}^{n_\theta} \theta_j(\hat{\mathsf{p}}) x_{ij}, \quad Y_i(\hat{\mathsf{p}}) = \sum_{j=1}^{n_\theta} \theta_j(\hat{\mathsf{p}}) y_{ij}$$

with x_{ij} and y_{ij} the optimization variables. Using this controller parametrization, the closed-loop transfer functions can be rewritten as

$$\mathcal{S}_{\mathsf{p}\hat{\mathsf{p}}} = \frac{Y_{\hat{\mathsf{p}}}}{Y_{\hat{\mathsf{p}}} + G_{\mathsf{p}} X_{\hat{\mathsf{p}}}},\ \mathcal{U}_{\mathsf{p}\hat{\mathsf{p}}} = \frac{X_{\hat{\mathsf{p}}}}{Y_{\hat{\mathsf{p}}} + G_{\mathsf{p}} X_{\hat{\mathsf{p}}}},\ \mathcal{T}_{\mathsf{p}\hat{\mathsf{p}}} = \frac{G_{\mathsf{p}} X}{Y_{\hat{\mathsf{p}}} + G_{\mathsf{p}} X_{\hat{\mathsf{p}}}} \tag{10}$$

The frequency set is defined as $\Omega := \Omega_{G_{\mathsf{p}}} \setminus B_{Y_{\hat{\mathsf{p}}}}$, where $B_{Y_{\hat{\mathsf{p}}}}$ is the set of frequencies corresponding to zeros of $Y_{\hat{\mathsf{p}}}$ on the unit circle. For conciseness, denote the common denominator of the closed-loop sensitivities

$$P_{\mathsf{p}\hat{\mathsf{p}}} = Y_{\hat{\mathsf{p}}} + G_{\mathsf{p}} X_{\hat{\mathsf{p}}} \tag{11}$$

3.1 Multi-objective synthesis

Soft $\mathcal{H}_2$ requirements: Similar to the problem formulation in Schuchert and Karimi (2023), the $\mathcal{H}_2$ synthesis problem can be reformulated as an optimization problem on the spectral norm as follows:

$$\min_{K_{\mathsf{p}}} \max_{\mathsf{p}\in\mathbb{P},\delta\in\mathbb{D}} \int_{-\pi}^{\pi} \mu_{\mathsf{p}\hat{\mathsf{p}}}(\omega) d\omega \tag{12a}$$

subject to

$$\left\| \begin{bmatrix} W_1(\omega)\mathcal{S}_{\mathsf{p}\hat{\mathsf{p}}}(e^{j\omega}) \\ W_2(\omega)\mathcal{U}_{\mathsf{p}\hat{\mathsf{p}}}(e^{j\omega}) \\ W_3(\omega)\mathcal{T}_{\mathsf{p}\hat{\mathsf{p}}}(e^{j\omega}) \end{bmatrix} \right\|^2 < \mu_{\mathsf{p}\hat{\mathsf{p}}}(\omega) \tag{12b}$$

$$\forall\omega \in \Omega, \forall\delta \in \mathbb{D}, \forall\mathsf{p} \in \mathbb{P}$$

where $\mu_{\mathsf{p}\hat{\mathsf{p}}}(\omega)$ is an upper bound of the (squared) Euclidean norm of the vector of the weighted sensitivity functions at ω, for a given (δ, p). The dependency on ω is again omitted in further equations when possible. The inequality in (12) can be rewritten using the sensitivities as expressed in (10), and multiplying both sides by $P^*_{\mathsf{p}\hat{\mathsf{p}}} P_{\mathsf{p}\hat{\mathsf{p}}}$, where $P_{\mathsf{p}\hat{\mathsf{p}}}$ is defined in (11):

$$\left\| \begin{bmatrix} W_1 Y_{\hat{\mathsf{p}}} \\ W_2 X_{\hat{\mathsf{p}}} \\ W_3 G_{\mathsf{p}} X_{\hat{\mathsf{p}}} \end{bmatrix} \right\|^2 < \mu_{\mathsf{p}\hat{\mathsf{p}}} P^*_{\mathsf{p}\hat{\mathsf{p}}} P_{\mathsf{p}\hat{\mathsf{p}}} \tag{13}$$

A linear lower bound of $P^*_{\mathsf{p}\hat{\mathsf{p}}} P_{\mathsf{p}\hat{\mathsf{p}}}$ can be derived around an arbitrary P_c:

$$\Phi_{\mathsf{p}\hat{\mathsf{p}}} := P^*_{\mathsf{p}\hat{\mathsf{p}}} P_c + P^*_c P_{\mathsf{p}\hat{\mathsf{p}}} - P^*_c P_c \le P^*_{\mathsf{p}\hat{\mathsf{p}}} P_{\mathsf{p}\hat{\mathsf{p}}}, \tag{14}$$

leading to a convex approximation of (13):

$$\min_{X_{\hat{\mathsf{p}}}, Y_{\hat{\mathsf{p}}}} \max_{\mathsf{p}\in\mathbb{P},\delta\in\mathbb{D}} \int_{-\pi}^{\pi} \mu_{\mathsf{p}\hat{\mathsf{p}}}(\omega) d\omega \tag{15a}$$

subject to

$$\left\| \begin{bmatrix} W_1 Y_{\hat{\mathsf{p}}} \\ W_2 X_{\hat{\mathsf{p}}} \\ W_3 G_{\mathsf{p}} X_{\hat{\mathsf{p}}} \end{bmatrix} \right\|^2 < \mu_{\mathsf{p}\hat{\mathsf{p}}} \Phi_{\mathsf{p}\hat{\mathsf{p}}} \tag{15b}$$

$$\Phi_{\mathsf{p}\hat{\mathsf{p}}}(\omega) > 0 \tag{15c}$$

$$\forall\omega \in \Omega, \forall\delta \in \mathbb{D}, \forall\mathsf{p} \in \mathbb{P}$$

Hard $\mathcal{H}_\infty$ requirements: Following the same steps as in the previous section, a similar convex constraint can be obtained for the hard $\mathcal{H}_\infty$ requirements. The $\mathcal{H}_\infty$ constraint is a constraint on the supremum of the singular value. For conciseness, only $\|\underline{W_1}\mathcal{S}\|_\infty < 1$ is detailed, which is reformulated as a set of constraints in the frequency domain:

$$\left| \underline{W_1}(\omega)\mathcal{S}_{\mathsf{p}\hat{\mathsf{p}}}(e^{j\omega}) \right|^2 < 1 \quad \forall\omega \in \Omega, \forall\delta \in \mathbb{D}, \forall\mathsf{p} \in \mathbb{P} \tag{16}$$

Dependency on ω is omitted hereafter when possible. Multiplying (16) by $P^*_{\mathsf{p}\hat{\mathsf{p}}} P_{\mathsf{p}\hat{\mathsf{p}}}$ and using the same lower bound as in (14) results in:

$$\left|\underline{W_1} Y_{\hat{\mathsf{p}}}\right|^2 < \Phi_{\mathsf{p}\hat{\mathsf{p}}} \quad \forall\omega \in \Omega, \forall\delta \in \mathbb{D}, \forall\mathsf{p} \in \mathbb{P} \tag{17}$$

Applying the same procedure on the other closed-loop transfer functions in (6) results in

$$\left|\underline{W_1} Y_{\hat{\mathsf{p}}}\right|^2 < \Phi_{\mathsf{p}\hat{\mathsf{p}}} \quad \left|\underline{W_2} X_{\hat{\mathsf{p}}}\right|^2 < \Phi_{\mathsf{p}\hat{\mathsf{p}}} \quad \left|\underline{W_3} G_{\mathsf{p}} X_{\hat{\mathsf{p}}}\right|^2 < \Phi_{\mathsf{p}\hat{\mathsf{p}}} \quad \forall\omega \in \Omega, \forall\delta \in \mathbb{D}, \forall\mathsf{p} \in \mathbb{P} \tag{18}$$

Similar constraints can be found when the synthesis objective is to minimize the $\mathcal{H}_\infty$ norm, or adding hard $\mathcal{H}_2$ requirements.

3.2 Stability

Formulating the $\mathcal{H}_2$ and $\mathcal{H}_\infty$ norm using bounds on the spectral norms is only possible when the closed-loop is stable. Stability analysis of the (frozen) LPV system is equivalent to stability analysis of an LTI system with uncertainty in the neighborhood of each operating point. With the correct choice of P_c, stability can be embedded in the problem formulation. Assume that an initial (possibly LPV) stabilizing controller $K_c = X_c Y_c^{-1}$ is known, and $Y_{\hat{\mathsf{p}}}$ and Y_c have the same degree. With the choice

$$P_c = Y_c + G_{\mathsf{p}} X_c, \tag{19}$$

a sufficient condition for stability is

$$P^*_{\mathsf{p}\hat{\mathsf{p}}} P_c + P^*_c P_{\mathsf{p}\hat{\mathsf{p}}} > 0 \quad \forall\omega \in \Omega, \forall\delta \in \mathbb{D}, \forall\mathsf{p} \in \mathbb{P} \tag{20}$$

which is enforced when $\Phi_{\mathsf{p}\hat{\mathsf{p}}} = P^*_{\mathsf{p}\hat{\mathsf{p}}} P_c + P^*_c P_{\mathsf{p}\hat{\mathsf{p}}} - P^*_c P_c \ge 0$.

If (20) holds, and if $Y_{\hat{\mathsf{p}}}$ and Y_c have the same order, then $1 + G_{\mathsf{p}} K_c$ and $1 + G_{\mathsf{p}} K_{\hat{\mathsf{p}}}$ have the same number of unstable zeros. Since K_c is a stabilizing controller, the closed-loop using $K_{\hat{\mathsf{p}}}$ is also stable. The stability proof can be found in Schuchert and Karimi (2023) when rewriting corresponding quantities using the fictitious operating point

$$\tilde{\mathsf{p}} = (\delta, \mathsf{p}) \in \mathbb{D} \times \mathbb{P}$$

and is therefore omitted. Note that stability for all fixed p implies stability for sufficient slow varying $\mathsf{p} = p(t)$ (Mohammadpour and Scherer, 2012).

4. IMPLEMENTATION CONSIDERATIONS

Similar remarks as in Karimi and Kammer (2017) and Schuchert and Karimi (2023) are in order, and given for completeness.

4.1 Gridding

The formulation (15) and (18) is a semi-infinite constraint, as it must be satisfied at every $\forall\omega \in \Omega, \forall\delta \in \mathbb{D}, \forall\mathsf{p} \in \mathbb{P}$. This is not feasible, but a common solution for such problems is to sample the frequencies, operating points and estimates at a sufficiently large number of points. At every sampled $(\omega, \delta, \mathsf{p})$, the convex constraint can be efficiently implemented using conic programming, in particular, rotated quadratic cones. This formulation allows using for a relatively dense gridding, as modern convex solvers can handle many second-order constraints used to implement (15) or (18).

When the $\mathcal{H}_2$ constraints are evaluated on a finite set of frequencies and operating points, a numerical integration scheme can be used to approximate the integral in (15a):

$$\int_{-\pi}^{\pi} \mu_{\mathsf{p}\hat{\mathsf{p}}}(\omega)d\omega \approx \frac{1}{2}\sum_{l=2}^{L}\left(\mu_{l,m,n} + \mu_{l,m-1,n}\right)\left(\omega_l - \omega_{l-1}\right)$$

and $\mu_{l,m,n} \geq 0$ a scalar optimization variable representing the value of $\mu_{\mathsf{p}\hat{\mathsf{p}}}(\omega)$ at $(\omega_l, \delta_m, \mathsf{p}_n)$.

4.2 Initial controller and iterative procedure

The proposed control design requires an initial (possibly LPV) stabilizing controller. Other structured synthesis approaches (Burke et al., 2006; Apkarian and Noll, 2006) also require this, and is used as an initial starting point for the optimization routines. It is reasonable to assume the existence of such a controller as

(1) For stable systems, any controller with a sufficiently small gain is stabilizing,
(2) For unstable systems, in a data-driven framework, a stabilizing controller required to collect input-output data.

The controller obtained after solving for the upper-bound of (4) using (15) and (17) will depend on the choice of K_c, and the resulting controller can be far away from the closest local minimum. It is proposed to solve the problem iteratively, using the optimal controller from the previous iteration as the initial controller for the next iteration, starting with K_c. Starting with the second iteration, the initial controller is always a feasible solution to the convex problem, and therefore the objective value achieved by the optimal controller is non-increasing. The final controller will converge to a local minimum, and conservatism from the convex-concave approximation will be small: $\Phi_{\mathsf{p}\hat{\mathsf{p}}} \approx P^*_{\mathsf{p}\hat{\mathsf{p}}} P_{\mathsf{p}\hat{\mathsf{p}}}$ when $P_{\mathsf{p}\hat{\mathsf{p}}} \approx P_c$.

Note that in the case of very demanding hard requirements, a feasible solution to (17) may not exist in the first iteration. If this is the case, it is proposed to first solve, possibly iteratively, the following sub-problem:

$$\min_{X_{\hat{\mathsf{p}}}, Y_{\hat{\mathsf{p}}}} \gamma$$

subject to

$$\left|\underline{W_1} Y_{\hat{\mathsf{p}}}\right|^2 < \gamma\Phi_{\mathsf{p}\hat{\mathsf{p}}} \quad \left|\underline{W_2} X_{\hat{\mathsf{p}}}\right|^2 < \gamma\Phi_{\mathsf{p}\hat{\mathsf{p}}} \quad \left|\underline{W_3} G_{\mathsf{p}} X_{\hat{\mathsf{p}}}\right|^2 < \gamma\Phi_{\mathsf{p}\hat{\mathsf{p}}}$$
$$\Phi_{\mathsf{p}\hat{\mathsf{p}}} > 0 \qquad \forall\omega \in \Omega, \forall\delta \in \mathbb{D}, \forall\mathsf{p} \in \mathbb{P}$$

If this converges to $\gamma = 0$, then the resulting controller can be used as initial controller for the original problem (4). If this converges to any $\gamma \neq 0$, a controller satisfying the hard requirements cannot be found from the initial starting point. Conflicting requirements may result in no (globally) feasible controller.

5. EXPERIMENTAL RESULTS

The proposed method is applied to the rotary table described in Section 2.

5.1 Coarse peak frequency estimator

During routine operation, performing a full spectral identification is too time-consuming, and therefore an estimator for $\hat{\mathsf{p}}$ must be derived, along with the uncertainty set $\mathbb{D}$ using a much shorter set of data. Since the system is linear at each frozen operating point, it is possible to obtain a reasonable estimate of the peak frequency using spectral analysis. Before inspecting a new object, an estimate of the peak frequency is obtained as follows: the rotary table (with the object on-top) is exited with random noise for 2 s, and input/output data collected. The power-spectrum of the input Φ_y and the output Φ_u is computed using Welch's method, and the peak frequency is computed as

$$\hat{\omega}_{\text{peak}} = \underset{65\leq\omega\leq137}{\arg\max} \, |\Phi_y(\omega)|/|\Phi_u(\omega)|$$

During an initial calibration phase, this procedure has been applied multiple times around different operating points, and each time, an accurate ω_{peak} also derived using a longer input/output sequence. From multiple experiments, it has been noted that $|\hat{\omega}_{\text{peak}} - \omega_{\text{peak}}| \leq 3$ with a probability over 95%. The set $\mathbb{D}$ is of uncertain operating point is here therefore chosen as $\mathbb{D} = [-3, 3]$.

5.2 Scheduling parameter

The controller's coefficients are parametrized as an affine combination of the scheduling vector θ. From (2), a good approximation of the transmission model is an affine dependency of the dynamics in the inertia, or equivalently an affine dependency on the inverse of the squared value of the peak frequency. The controller is therefore scheduled with a similar dependency: $\theta = [1, \hat{\omega}^{-2}_{\text{peak}}]$. Other scheduling parameters are possible, but it has been noted that more complicated scheduling vectors do not result in a significant increase in performance. To showcase the benefits of the proposed approach over state-of-the-art synthesis methods, comparison with an LTI robust controller will be given. This controller is obtained using the approach proposed in Karimi and Kammer (2017), treating the uncertain LPV dynamics as multi-model uncertainty, and is equivalent in the proposed formulation to using the scheduling vector $\theta = 1$.

5.3 Controller design

To decide about the controller order, different robust controllers have been designed using increasing orders. After order $n = 8$, little improvements are noticed, and therefore this order is chosen. For the comparison, the LPV controller is also chosen to be of order 8.

The design objective is to minimize the (squared) tracking error given a ramp reference. This can be formulated as minimizing $\|W_1 \mathcal{S}_{\mathsf{p}\hat{\mathsf{p}}}\|_2$ where $W_1 = 1/(z-1)^2$, and following the definition in (5), $W_2 = W_3 = 0$.

Hard requirements are specified to guarantee additional specifications during routine operation. A modulus margin of 0.5 is required, resulting in $\underline{W_1} = 2$. To avoid passing the large high-frequency components to the inner-loop, a constraint is added to the input sensitivity function $\mathcal{U}_{\mathsf{p}\hat{\mathsf{p}}}$ corresponding to

$$\underline{W_2} = \begin{cases} 0 & \omega \leq 360 \\ -90\text{dB} & \text{otherwise} \end{cases}$$

A final constraint is used to limit the amplitude of the complementary sensitivity function $\mathcal{T}_{\mathsf{p}\hat{\mathsf{p}}}$, and corresponds to the filter $\underline{W_3} = 0.5$. The initial stabilizing controller is chosen as

$$K_c = 100 + \frac{10}{z-1} = \frac{100z^8 - 90z^7}{z^8 - z^7}$$

and $F_y = z - 1$ is used as a fixed part in the denominator. The problem is solved using the frequency grid from the FRF, the operating points at 25 different points, and $\mathbb{D}$ gridded such that $\delta \in \{-3, -1.5, 0, 1.5, 3\}$. The control synthesis is iterated until convergence to a local minimum. The resulting controller, sampled at a linearly spaced grid p is shown in Fig. 4, and the closed-loop transfer functions, given at $\hat{\mathsf{p}} = \mathsf{p}$, along with (the inverse of) the weighting function $\underline{W_i}$ in Fig. 5. The closed-loop transfer functions using the robust controller are also given in this figure.

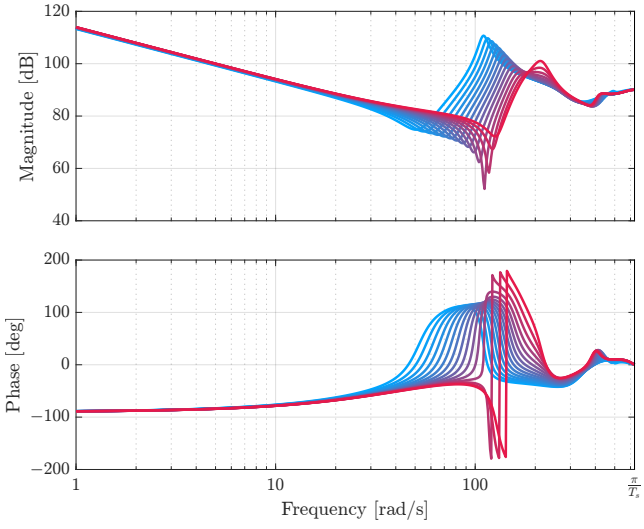

Fig. 4. Frequency response of the controller at different operating points, using the same color-code as Fig. 3.

From Fig. 5a, it is clearly visible the benefit of this LPV controller w.r.t a robust controller. The sensitivity is about 6 dB lower in low frequencies, while satisfying the same design requirements. To showcase time-domain improvement

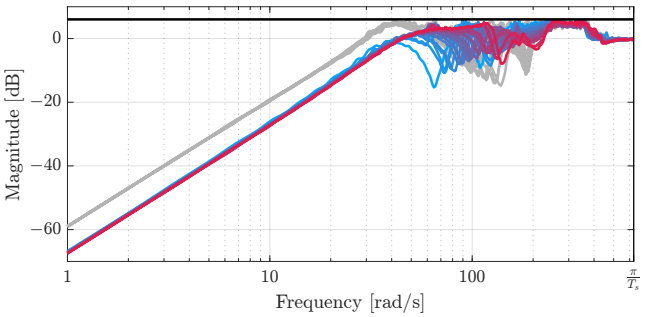

(a) Sensitivity $\mathcal{S}_{\mathsf{p}\hat{\mathsf{p}}}$ and $\underline{W_1}^{-1}$

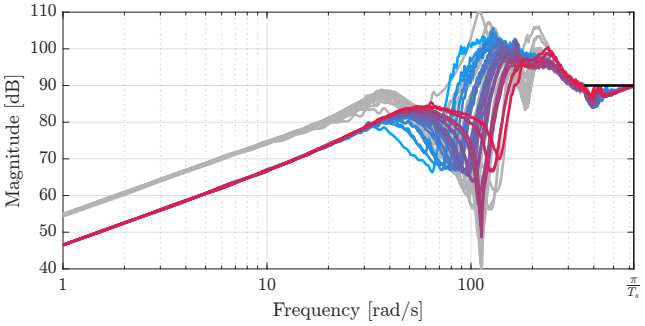

(b) Input sensitivity $\mathcal{U}_{\mathsf{p}\hat{\mathsf{p}}}$ and $\underline{W_2}^{-1}$

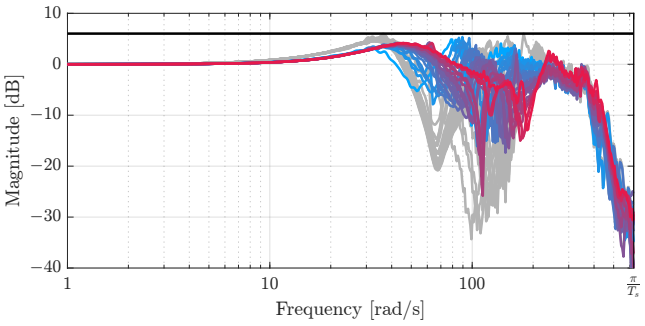

(c) Complementary sensitivity $\mathcal{T}_{\mathsf{p}\hat{\mathsf{p}}}$ and $\underline{W_3}^{-1}$

Fig. 5. Closed-loop transfer function using LPV controller in color, using the same color-code as Fig. 3. Closed-loop transfer functions using a robust controller, shown in gray.

in performance, the rotary-table is tasked with tracking the reference shown in Fig. 6. Note that for the desired application, the reference is only slowly changing, and performance mostly dictated by low-frequency behavior of $\mathcal{S}_{\mathsf{p}\hat{\mathsf{p}}}$. The tracking error using either the LPV or robust controller is shown in Fig. 7. As it can be seen, the LPV controller improves tracking performance, for this trajectory, by a factor ≈ 2 ($= 6\,\text{dB}$).

6. CONCLUSION

We have presented a novel approach to the design of LPV controllers for SISO systems with uncertain scheduling parameters. The local frequency response of the system is used to design an LPV controller, locally optimal to a multi-objective mixed-sensitivity problem. This method is applied to a rotary table, where improved performance has been obtained w.r.t. a state-of-the-art controller.

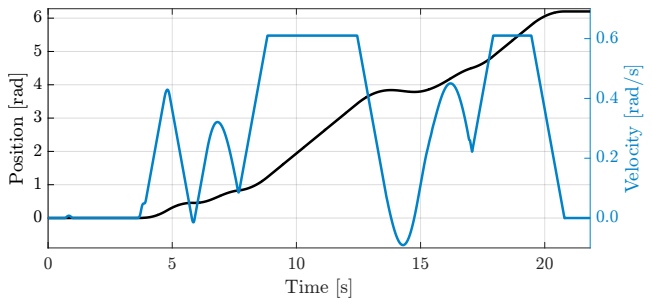

Fig. 6. Reference trajectory obtained from inspecting an object. For the specific inspection application, velocity, and acceleration are limited

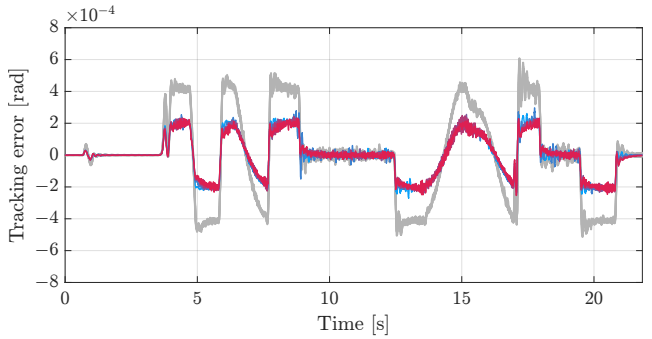

Fig. 7. Tracking error around different operating points using LPV, shown in color. Tracking error using the robust controller, shown in gray.

REFERENCES

Agulhari, C.M., Tognetti, E.S., Oliveira, R.C., and Peres, P.L. (2013). $\mathcal{H}_\infty$ dynamic output feedback for LPV systems subject to inexactly measured scheduling parameters. In *2013 American control conference*, 6060–6065.

Apkarian, P. and Noll, D. (2006). Nonsmooth $\mathcal{H}_\infty$ synthesis. *IEEE Trans. on Automatic Control*, 51(1), 71–86.

Bloemers, T., Oomen, T., and Tóth, R. (2021). Frequency response data-driven LPV controller synthesis for MIMO systems. *IEEE Control Systems Letters*, 6, 2264–2269.

Bloemers, T., Tóth, R., and Oomen, T. (2019a). Towards data-driven LPV controller synthesis based on frequency response functions. *Proceedings of the IEEE Conference on Decision and Control*, 2019-December, 5680–5685.

Bloemers, T., Tóth, R., and Oomen, T. (2019b). Data-driven LPV reference tracking for a control moment gyroscope. *IFAC-PapersOnLine*, 52, 134–139.

Burke, J.V., Henrion, D., Lewis, A.S., and Overton, M.L. (2006). HIFOO-a MATLAB package for fixed-order controller design and $\mathcal{H}_\infty$ optimization. *IFAC Proceedings Volumes*, 39(9), 339–344.

da Silva, M.M., Brüls, O., Swevers, J., Desmet, W., and Van Brussel, H. (2009). Computer-aided integrated design for machines with varying dynamics. *Mechanism and Machine Theory*, 44(9), 1733–1745.

Dong, L., Tang, W., and Bao, D. (2015). Interpolating gain-scheduled $\mathcal{H}_\infty$ loop shaping design for high speed ball screw feed drives. *ISA Transactions*, 55, 219–226.

Hoffmann, C. and Werner, H. (2015). A survey of linear parameter-varying control applications validated by experiments or high-fidelity simulations. *IEEE Transactions on Control Systems Technology*, 23, 416–433.

Karimi, A. and Emedi, Z. (2013). $\mathcal{H}_\infty$ gain-scheduled controller design for rejection of time-varying disturbances with application to an active suspension system. *Proceedings of the IEEE Conference on Decision and Control*, 7540–7545.

Karimi, A. and Kammer, C. (2017). A data-driven approach to robust control of multivariable systems by convex optimization. *Automatica*, 85, 227–233.

Kose, I.E. and Jabbari, F. (1999). Control of LPV systems with partly measured parameters. *IEEE Transactions on Automatic Control*, 44(3), 658–663.

Kunze, M., Karimi, A., and Longchamp, R. (2007). Gain-scheduled controller design by linear programming. In *2007 European Control Conference (ECC)*, 5432–5438.

Mohammadpour, J. and Scherer, C.W. (2012). *Control of linear parameter varying systems with applications*. Springer Science & Business Media.

Oomen, T. (2018). Advanced motion control for precision mechatronics: Control, identification, and learning of complex systems. *IEEJ Journal of Industry Applications*, 7, 127–140.

Paijmans, B., Symens, W., Brussel, H.V., and Swevers, J. (2006). A gain-scheduling-control technique for mechatronic systems with position-dependent dynamics. *2006 American Control Conference*, 2934–2938.

Pintelon, R. and Schoukens, J. (2012). *System Identification: A Frequency Domain Approach*. Wiley.

Rugh, W.J. and Shamma, J.S. (2000). Research on gain scheduling. *Automatica*, 36, 1401–1425.

Sato, M., Ebihara, Y., and Peaucelle, D. (2010). Gain-scheduled state-feedback controllers using inexactly measured scheduling parameters: $\mathcal{H}_2$ and $\mathcal{H}_\infty$ problems. In *Proceedings of the 2010 American Control Conference*, 3094–3099.

Schuchert, P. and Karimi, A. (2023). Frequency-domain data-driven position-dependent controller synthesis for cartesian robots. *IEEE Transactions on Control Systems Technology*. doi:10.1109/TCST.2023.3257487.

Steinbuch, M., van de Molengraft, M., and Van Der Voort, A.J. (2003). Experimental modelling and LPV control of a motion system. In *Proceedings of the 2003 American control conference, ACC: June 4-6, 2003, Denver, Colorado, USA. Vol. 2*, 1374–1379. Institute of Electrical and Electronics Engineers.

Symens, W., Brussel, H.V., and Swevers, J. (2004). Gain-scheduling control of machine tools with varying structural flexibility. *CIRP Annals*, 53, 321–324.

Tóth, R. (2010). *Modeling and Identification of Linear Parameter-Varying Systems*. Springer.

Tóth, R., van de Wal, M., Heuberger, P.S., and Van den Hof, P.M. (2011). LPV identification of high performance positioning devices. In *Proceedings of the 2011 American Control Conference*, 151–158.

Wassink, M.G., van de Wal, M., Scherer, C., and Bosgra, O. (2005). LPV control for a wafer stage: beyond the theoretical solution. *Control Engineering Practice*, 13(2), 231–245.